Cell PRESS
Open ACCESS

Cell Reports
Article

Dendritic Cells Coordinate Innate Immunity via MyD88 Signaling to Control *Listeria monocytogenes* Infection

Catharina Arnold-Schrauf,[1] Markus Dudek,[1] Anastasia Dielmann,[1] Luigia Pace,[2] Maxine Swallow,[1] Friederike Kruse,[1] Anja A. Kühl,[3] Bernhard Holzmann,[4] Luciana Berod,[1,5] and Tim Sparwasser[1,5,*]

[1]Institute for Infection Immunology, TWINCORE, Center for Experimental and Clinical Infection Research, a Joint Venture between the Medical School Hannover (MHH) and the Helmholtz Center for Infection Research (HZI), 30625 Hannover, Germany
[2]Institut National de la Santé et de la Recherche Médicale (INSERM) U932, Institut Curie, 75005 Paris, France
[3]Department of Medicine I for Gastroenterology, Infectious Disease and Rheumatology, Campus Benjamin Franklin, Charité-Universitätsmedizin Berlin, 12203 Berlin, Germany
[4]Chirurgische Klinik und Poliklinik, Technische Universität München, 81675 Munich, Germany
[5]These authors contributed equally to this work
*Correspondence: sparwasser.tim@mh-hannover.de
http://dx.doi.org/10.1016/j.celrep.2014.01.023

SUMMARY

Listeria monocytogenes **(LM), a facultative intracellular Gram-positive pathogen, can cause life-threatening infections in humans. In mice, the signaling cascade downstream of the myeloid differentiation factor 88 (MyD88) is essential for proper innate immune activation against LM, as MyD88-deficient mice succumb early to infection. Here, we show that MyD88 signaling in dendritic cells (DCs) is sufficient to mediate the protective innate response, including the production of proinflammatory cytokines, neutrophil infiltration, bacterial clearance, and full protection from lethal infection. We also demonstrate that MyD88 signaling by DCs controls the infection rates of CD8α$^+$ cDCs and thus limits the spread of LM to the T cell areas. Furthermore, in mice expressing MyD88 in DCs, inflammatory monocytes, which are required for bacterial clearance, are activated independently of intrinsic MyD88 signaling. In conclusion, CD11c$^+$ conventional DCs critically integrate pathogen-derived signals via MyD88 signaling during early infection with LM in vivo.**

INTRODUCTION

Infections with the food-borne Gram-positive facultative intracellular bacterium *Listeria monocytogenes* (LM) can result in systemic bacteraemia and high mortality rates in immunocompromised patients. In mice, the systemic infection model of listeriosis has provided valuable insights into host-pathogen interactions. Although both a functional innate response and an adaptive immune response are critical for eradicating the pathogen, the innate response is particularly important for containing bacterial replication and spread. Innate immune cells, such as neutrophils, inflammatory monocytes, so-called tumor necrosis factor (TNF)/inducible NO synthase (iNOS)-producing dendritic cells (TipDCs), macrophages, natural killer (NK) cells, NKT cells, and conventional DCs (cDCs) cooperate to form a protective line of defense early after infection (Stavru et al., 2011; Williams et al., 2012). cDCs provide an important early source of interleukin-12 (IL-12), which in turn induces interferon γ (IFNγ) release by NK, NKT, and T cells (Kang et al., 2008; Zhan et al., 2010). The innate response is also characterized by a fast infiltration of neutrophils and TipDCs to the spleen and liver. In addition, resident macrophages as well as TipDCs mediate pathogen clearance via effector mechanisms based on reactive oxygen or nitrogen species and TNF-α (Pamer, 2004). In this process, IFNγ enhances macrophage activation and is critical for the differentiation of monocyte-derived TipDCs, which are required for LM clearance (Kang et al., 2008; Serbina et al., 2003b; Shi et al., 2011).

A broad range of phagocytes are infected early during inoculation with LM, including marginal zone (MZ) macrophages, metallophilic macrophages, cDCs, and neutrophils (all located in the MZ of the spleen), as well as F4/80$^+$ red pulp macrophages (Aoshi et al., 2008, 2009; Waite et al., 2011). Macrophages and neutrophils are highly efficient in killing bacteria (Stavru et al., 2011), whereas cDCs have a reduced microbicidal activity as compared with macrophages in vitro (Alaniz et al., 2004). Thus, cDCs seem to provide a favorable environment for bacterial survival. In addition, cDCs, rather than macrophages present in the MZ, are required for LM infection of the T cell areas, where T cell priming occurs (Aoshi et al., 2008). In contrast to neutrophils and red pulp macrophages, CD8α$^+$ cDCs, a subset of cDCs with specific functions in cross-presentation, are the primary reservoir for live bacteria, and there is evidence that CD8α$^+$ cDCs can shuttle live LM from the MZ to the T cell areas (Campisi et al., 2011;

Neuenhahn et al., 2006; Verschoor et al., 2011). Furthermore, *Batf3*$^{-/-}$ mice, which lack CD8α^+ cDCs, show a clear correlation between the absence of this subset and a reduced bacterial burden upon LM infection (Edelson et al., 2011). Conversely, both Flt3 ligand (Flt3L)-treated mice and mice carrying a DC-specific deletion of the phosphatase and tensin homolog (Pten), a negative regulator of Flt3L signaling, exhibit an increase in CD8α^+ cDC numbers and higher infection rates in the spleen (Alaniz et al., 2004; Sathaliyawala et al., 2010).

Innate signaling via the adaptor molecule myeloid differentiation factor 88 (MyD88) is essential during pathogen recognition of LM, since *Myd88*$^{-/-}$ mice are highly susceptible to LM infection and die before a protective adaptive immune response can be mounted (Edelson and Unanue, 2002; Seki et al., 2002). MyD88 controls downstream signaling of most Toll-like receptors (TLRs), except for TLR3 and in part TLR4, as well as the IL-1R family (Akira and Takeda, 2004). *Myd88*$^{-/-}$ mice display defective innate immune responses, including absence or low levels of proinflammatory cytokines such as IL-12, IFNγ, IL-6, and IL-18, as well as an impaired neutrophil recruitment, enhanced lymphocyte apoptosis in the splenic white pulp, and a strongly increased bacterial burden in both spleen and liver (Edelson and Unanue, 2002; Seki et al., 2002; Serbina et al., 2003a; Torres et al., 2004). Furthermore, TipDC activation for efficient bacterial killing is dysfunctional in *Myd88*$^{-/-}$ mice (Serbina et al., 2003a). Given the broad expression of MyD88, the extent to which MyD88 signaling in different cell types contributes to control of LM infection is unknown. Also, despite their contribution to bacterial dissemination, it is likely that CD8α^+ cDCs have evolved mechanisms to restrict bacterial replication or survival. To date, it is unclear whether MyD88 signaling by CD8α^+ cDCs is part of such a cell-intrinsic protection mechanism against LM infection in vivo. Moreover, MyD88 signaling has been an attractive target for new vaccination and immunotherapy strategies for several years (Connolly and O'Neill, 2012). Yet, its widespread expression and the lack of experimental models for specifically targeting MyD88 in defined cell subsets have hindered efforts to understand its contribution to the innate immune responses against pathogens.

In this study, we used a mouse model in which MyD88 expression is confined to CD11c$^+$ cells. Our results show that MyD88 signaling by DCs is sufficient to revert the defective innate immune response observed in MyD88-deficient mice to wild-type (WT) levels by controlling both the bacterial burden in the infected organs as well as the infection rates of CD8α^+ cDCs early during pathogen encounter. At the same time, MyD88 signaling in TipDCs is dispensable for their activation in vivo. Thus, cDCs critically regulate the activation of innate immunity against LM via MyD88 signaling.

RESULTS

A Mouse Model for Switching on MyD88 Signaling by DCs In Vitro and In Vivo

To study the role of MyD88 signaling by DCs, we used a mouse model in which MyD88 expression is specifically restricted to CD11c$^+$ cells. For this purpose, we crossed MyD88stop mice (termed Mst mice), which carry a disruptive stop cassette in the *Myd88* locus and do not express the MyD88 protein (Gais et al., 2012), to CD11c (*Itgax*) Cre mice (Caton et al., 2007) expressing Cre recombinase under the control of the *Itgax* promoter (termed ItgaxCre mice). The resulting ItgaxMst mice were homozygous for the stop cassette and transgenic for Cre, thereby allowing only CD11c$^+$ cells to switch on *Myd88* gene expression.

First, we tested the functionality of MyD88 signaling by DCs in ItgaxMst mice by assessing the upregulation of activation markers, including CD80, CD86, and CD40, as well as the cytokine production by bone marrow (BM)-derived DCs and ex vivo isolated cDCs upon stimulation. *Mycobacterium tuberculosis* (*Mtb*) or *Candida albicans* (CA) can also trigger MyD88-independent pattern recognition receptors (PRR) (Akira and Takeda, 2004; van den Berg et al., 2012), and DC activation occurred in WT, ItgaxMst, and Mst BM-derived DCs in vitro (Figure 1A). In contrast, CpG-B, a well-known TLR9 agonist (Hemmi et al., 2000; Sparwasser and Lipford, 2000), as well as LM, induced the upregulation of CD80 expression in WT and ItgaxMst DCs to comparable levels, whereas Mst DCs showed impaired upregulation of this marker (Figures 1A and S1A). In addition, BM-derived Mst DCs were only responsive to MyD88-independent activation with respect to IL-12p40 production, whereas WT and ItgaxMst ex vivo DCs produced similar amounts of this cytokine upon stimulation with the tested PRR agonists in vitro (Figures 1B and S1B). Moreover, cDCs from mice treated with CpG-B or PBS in vivo were tested for CD86 and CD40 upregulation. cDCs from CpG-B-injected Mst mice showed CD86/CD40 expression levels comparable to the PBS controls from all genotypes (Figure 1C and data not shown). In contrast, the same level of upregulation of both markers was observed upon CpG-B injection in WT and ItgaxMst cDCs (Figure 1C). Also, CpG-B-triggered IL-6 and TNF-α serum levels were similarly induced in WT and ItgaxMst mice, whereas Mst mice did not respond to this stimulation (Figure 1D). Taken together, these results demonstrate that DCs from ItgaxMst mice show reactivation of the MyD88-dependent TLR signaling pathways, which is absent in Mst mice, both in vitro and in vivo.

MyD88 Signaling by DCs Is Sufficient to Trigger the Early Innate Response against LM Infection

Myd88$^{-/-}$ mice infected with LM display multiple defects in the early events of the innate immune response, such as a lack of inflammatory cytokines and a defective neutrophilic infiltration, that contribute to the high bacterial burden (Edelson and Unanue, 2002; Seki et al., 2002). The widespread expression of MyD88 by all innate immune cells, as well as the early death of infected mice, has limited our understanding of the role of MyD88 during LM infection.

To test whether MyD88 signaling by DCs was sufficient to revert early defects of the innate immune response, we first analyzed IFNγ and IL-6 serum levels in WT, ItgaxMst, and Mst mice at 24 hr postinfection (hpi). We found comparable IFNγ and IL-6 serum levels in WT and ItgaxMst mice (Figure 2A). Also, similar expression of IL-12p40 by cDCs from WT and ItgaxMst mice was observed (Figure S2A). In contrast, serum IFNγ and IL-6 were not detectable and cDCs did not express IL-12p40 in infected Mst mice (Figures 2A and S2A).

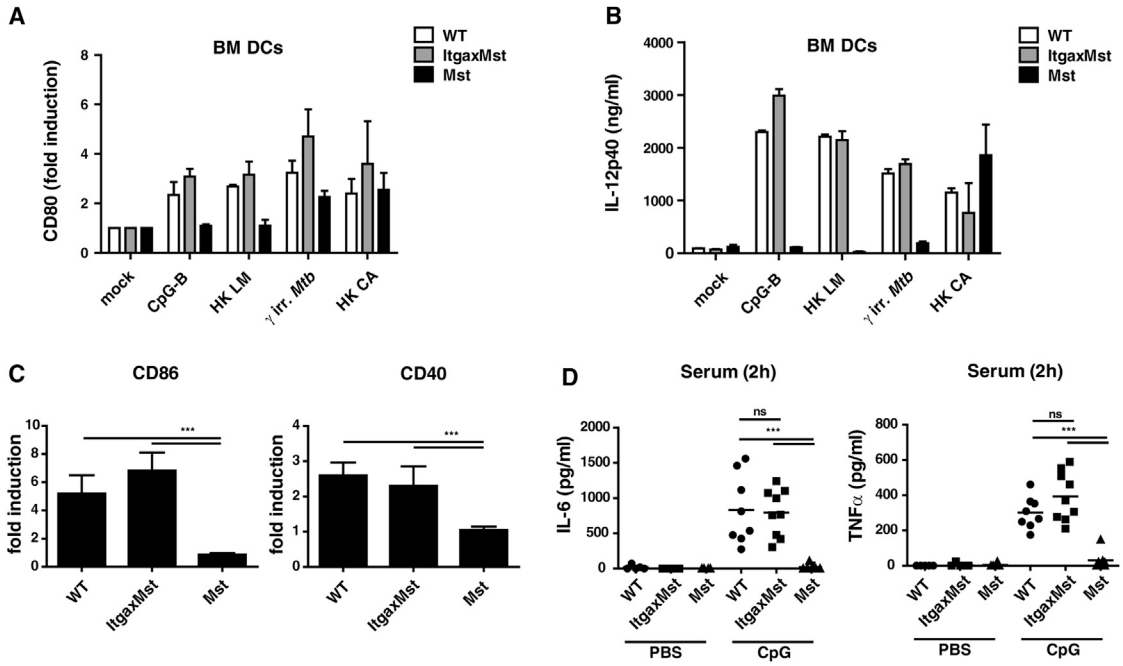

Figure 1. MyD88 Signaling in ItgaxMst Mice Is Functional In Vitro and In Vivo

(A) GM-CSF DCs were treated with the indicated stimuli in triplicate in vitro and analyzed for the upregulation of CD80 by flow cytometry 24 hr later. Heat-killed (HK) LM, *Candida albicans* (CA), γ-irradiated *Mycobacterium tuberculosis* (γ irr. *Mtb*). Fold induction of the MFI for CD80 is displayed as the mean value + SD from pooled data from three independent experiments.

(B) IL-12p40 production by the stimulated cells from (A) was determined by ELISA. Data are shown as the mean + SD from triplicate stimulations from one representative experiment out of three.

(C) Mice (n = 4/group) were injected with CpG-B or PBS i.p., and CD86/CD40 upregulation by $CD11c^{hi}MHCII^{hi}$ cDCs was tested 12 hr later. Data are displayed as mean fold induction + SD over the PBS control.

(D) Serum levels for IL-6 and TNF-α from (C) were analyzed 2 hr after treatment. Data for individual mice are displayed. Bars indicate mean values. The experiments shown in (C) and (D) were performed twice with comparable results. Statistics were calculated by one-way ANOVA. ns, not significant.

See also Figure S1.

Interestingly, when we compared cDC subsets for their IL-12p40 production, we found that mainly $CD8\alpha^+$ cDCs produced this cytokine at 12 hpi, whereas IL-12 production by $CD8\alpha^-$ cDCs was at the level observed in the uninfected mice (Figures 2B and 2C). At 24 hpi, $CD11b^+$ cDCs became the main source of IL-12p40 (Figures S2B and S2C), consistent with published data (Tam and Wick, 2006). Furthermore, the defective neutrophilic infiltration in the spleen of infected Mst mice was completely reverted in ItgaxMst mice (Figures 2D and 2E).

Early after infection, LM preferentially localizes to the T cell area, where it starts to proliferate exponentially (Aoshi et al., 2008). Thus, we next tested whether ItgaxMst mice can control the bacterial burden upon LM infection. Indeed, the bacterial loads in the spleen and liver of both WT and ItgaxMst mice were comparable at 24 and 72 hpi, as opposed to Mst mice, which showed significantly increased colony-forming units (cfu) at both time points (Figures 3A and 3B). *Myd88*$^{-/-}$ mice suffer from high T cell area infection rates as compared with WT mice (Edelson and Unanue, 2002). Accordingly, when we infected Mst mice with LM expressing the red fluorescent protein (LM RFP) (Waite et al., 2011), we observed significantly increased infection rates in the T cell areas of Mst mice at 24 hpi as compared with WT mice. Conversely, the ItgaxMst and WT mice showed comparably low infection rates (Figures 3C and 3D). Finally, we wanted to assess the consequences of this early control of bacterial replication and spread for survival by monitoring LM-infected WT, ItgaxMst, and Mst mice over a period of 14 days (Figure 3E). As expected, Mst mice died early after infection. In contrast, both WT and ItgaxMst mice survived. Thus, the targeted expression of MyD88 by DCs is sufficient to revert the detrimental defects of the innate immune response and prevent the uncontrolled replication of bacteria as observed in Mst mice.

MyD88 Signaling Controls the Niche Size for Live LM, but Is Dispensable for Limiting Bacterial Replication in $CD8\alpha^+$ cDCs

Since ItgaxMst mice display a better control of bacterial replication compared with Mst mice, we questioned whether this might be influenced by differences in the infection rates of cDCs. In particular, $CD8\alpha^+$ cDCs provide a favorable niche for live LM early during infection, and the splenic bacterial load is critically dependent on $CD8\alpha^+$ cDC numbers (Alaniz et al., 2004; Campisi et al., 2011; Edelson et al., 2011; Neuenhahn et al., 2006; Satha-liyawala et al., 2010). However, the influence of MyD88 signaling by DCs on LM numbers within individual innate cell populations,

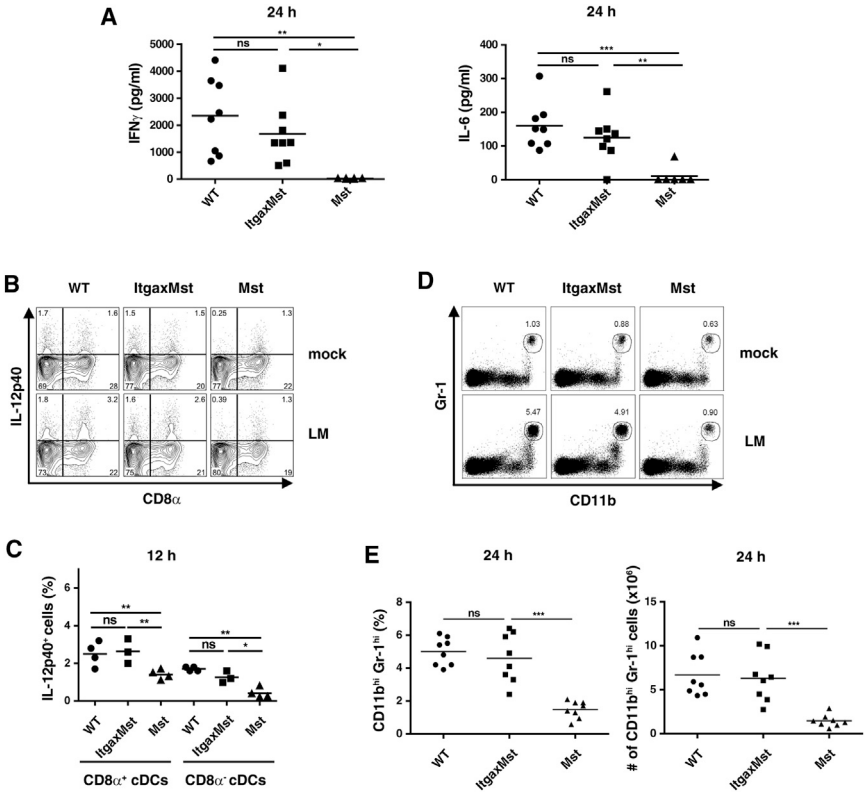

Figure 2. MyD88 Signaling by DCs Is Sufficient to Revert Early Defects in the Innate Response against LM

Mice were infected with LM for 12 hr (B and C) or 24 hr (A, D, and E).

(A) IFNγ and IL-6 serum levels were analyzed.

(B) Plots show the frequency of IL-12p40$^+$ CD8α$^+$ or CD8α$^-$ cDCs from the spleen of uninfected (mock) or infected (LM) mice in the live CD11c^{hi} gate after in vitro culture in the presence of Golgi Plug.

(C) Quantification of (B). Bars indicate mean values. Experiments were performed twice.

(D) Splenic neutrophils from mock-treated or LM-infected mice were gated as Gr-1^{hi}CD11b^{hi} live cells.

(E) Quantification of the frequency and total numbers of neutrophils from infected mice shown in (D). Symbols represent individual mice pooled from two experiments. Bars indicate mean values. Neutrophil numbers were comparable in uninfected mice from all tested genotypes (mean value/spleen = 1.2 × 10^6 cells; data not shown). Statistics were calculated by one-way ANOVA. ns, not significant.

See also Figure S2.

including neutrophils, monocytes, macrophages, NK cells, CD8α$^-$ cDCs, and CD8α$^+$ cDCs, is unknown. First, we checked the initial uptake or early replication of LM. At 3 hpi, CD8α$^+$ cDCs were the only infected population (Figure 4A), consistent with published data obtained in WT mice (Neuenhahn et al., 2006). CD8α$^+$ cDC numbers were comparable in all tested genotypes prior to infection (Figures S3A and S3B). We also found no significant differences in the bacterial numbers per 10^3 cells or bacterial burden per spleen between the genotypes at 3 hpi (Figure 4B). At 15 hpi, we further observed infection in CD8α$^-$ cDCs and neutrophils/monocytes/macrophages. NK cell infection was close to the detection limit of this assay for all genotypes tested. Interestingly, the number of live bacteria was higher for all cell populations in Mst mice. In contrast, WT and ItgaxMst mice showed similar infection rates (Figure 4C). Also, the bacterial burden per spleen was increased in Mst mice. By contrast, WT and ItgaxMst mice exhibited comparable splenic infection rates (Figure 4D).

To study whether the enhanced CD8α$^+$ cDC infection rates in Mst mice are due to a defective DC functionality or caused by the increased bacterial burden observed in these mice, we next examined the size of the bacterial niche in CD8α$^+$ cDCs from mixed BM chimeras. Mixed BM chimeras permit a direct comparison of the infection rates of WT and Mst CD8α$^+$ cDCs in the same in vivo environment. We performed experiments at 9 hpi to minimize indirect effects of the WT on MyD88-deficient DCs. We generated mixed BM chimeras by transferring Mst CD45.1$^-$ and WT CD45.1$^+$ or Mst GFP$^-$ and Mst CD11cCre-GFP GFP$^+$ (CD11cCre-GFP mice crossed to Mst mice) BM cells into Mst recipients. CD8α$^+$ or CD8α$^-$ cDC populations were separated according to CD45.1 or GFP expression upon infection (Figure 4E). We found slightly increased infection rates per 10^3 cells in Mst CD8α$^+$ cDCs as compared with WT or Mst CD11cCre-GFP cDCs (Figure 4F). No bacteria could be detected in CD8α$^-$ cDCs (data not shown). Also, MyD88 did not influence the bacterial replication in or killing by ex vivo CD8α$^+$ cDCs infected with LM in vitro (Figures S3C–S3E). Thus, MyD88 signaling plays a minor role in limiting the bacterial replication of LM in CD8α$^+$ cDCs in vivo and in vitro. Taken together, these results indicate that MyD88 signaling by DCs controls the bacterial burden in CD8α$^+$ cDCs in vivo mainly by reducing the overall splenic infection rate.

TipDCs Do Not Require Cell-Intrinsic MyD88 Signaling for Their Activation

To better understand how ItgaxMst mice control early bacterial replication upon LM infection, we analyzed TipDC activation. TipDCs are critical innate cells for limiting the bacterial burden during LM infection, as their depletion during the first days of infection results in high bacterial replication and death (Serbina et al., 2003b; Shi et al., 2011). TipDC activation for the production of the critical effector molecules TNF-α and NO is defective in *Myd88*$^{-/-}$ mice (Serbina et al., 2003a), yet it is unknown whether MyD88 signaling is required by TipDCs intrinsically. To examine this issue, we used infected WT, ItgaxMst, and Mst mice at 24 hpi. An increase in CD11b^{int}Ly-6C^{hi} Mac-3^{hi} cells was detectable in all mice upon infection, although it was significantly lower in Mst mice (Figures 5A, 5B, and S4). TipDC activation, as assessed by intracellular iNOS and TNF-α staining, was defective in Mst mice (Figures 5C and 5D) consistent with published

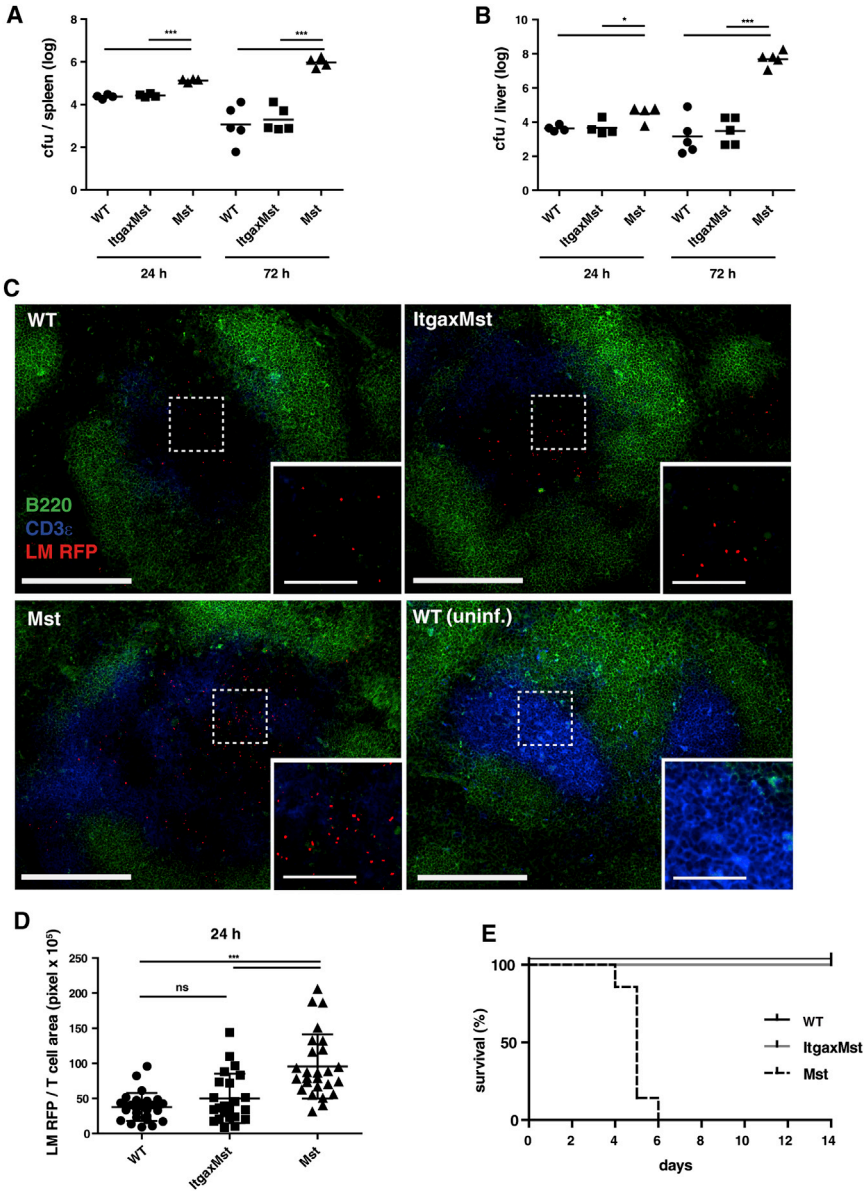

Figure 3. The Spread of Infection to the T Cell Areas Is Limited by MyD88 Signaling

Mice were infected with LM (A, B, and E) or LM RFP (C and D).

(A and B) The bacterial burden in spleen (A) and liver (B) was determined at 24 and 72 hpi. Experiments were performed two to three times with comparable results. Bars indicate mean values. Statistics were calculated by one-way ANOVA.

(C) Cryosections from the spleens of LM RFP-infected WT, ItgaxMst, Mst, and uninfected mice were stained for CD3ε and B220 at 24 hpi. Representative immunofluorescence pictures from three mice per group are shown. Scale bars correspond to 200 μm. Dashed lines indicate the border of the inset depicted in the right corner of each low-power view. Scale bar in insets, 50 μm.

(D) Quantification of the histology shown in (C) from 23–27 individual T cell areas per genotype. The T cell area was defined as the $B220^-$ area inside the B cell follicle. The numbers of RFP pixels/total pixels of the T cell area were quantified and multiplied by 10^5 for better readability. Bars indicate mean ± SD. Statistics were calculated by using the Kruskal-Wallis test. ns, not significant.

(E) Survival of mice (n = 7–8 mice/group) was checked daily over a period of 14 days. The experiment was performed three times. The differences in survival between the Mst and WT or ItgaxMst mice were significant ($p < 0.001$) as calculated by the log rank test.

data (Serbina et al., 2003a). In contrast, TipDCs in ItgaxMst and WT mice produced similar amounts of iNOS and TNF-α (Figures 5C and 5D). Surprisingly, although TipDCs are known to upregulate CD11c expression during activation (Serbina et al., 2003b), most TipDCs were still $CD11c^-$ at 24 hpi (Figure 5E). The CD11c promoter activity mediates Cre-driven excision of the *Myd88stop* cassette and thereby determines the reactivation of MyD88 signaling in ItgaxMst mice. Thus, we analyzed *Myd88* mRNA expression by TipDCs from infected WT and ItgaxMst mice at 24 hpi. Indeed, low CD11c surface expression correlated with minor *Myd88* expression (9.9% ± 1.1%) by TipDCs from ItgaxMst as compared with WT mice, whereas cDCs isolated from both mice expressed the same levels of *Myd88* mRNA. Cells isolated from Mst mice did not contain *Myd88* mRNA (Figure 5F). Thus, at 24 hpi the majority of TipDCs in ItgaxMst mice are MyD88 deficient, yet their activation is comparable to that observed in WT mice. We propose a mechanism by which DCs control TipDC activation during LM infection in an indirect, MyD88-dependent fashion.

DISCUSSION

The high susceptibility of $Myd88^{-/-}$ mice to LM infection demonstrates the central importance of the MyD88 signaling cascade for the induction of a protective immune response (Seki et al., 2002). Yet, less is known about the cell-type-specific role of MyD88 signaling. In this study, we demonstrate that MyD88 signaling by DCs is sufficient to control the overall bacterial burden and thus prevent dissemination of bacteria to the T cell areas.

LM exploits $CD8\alpha^+$ cDCs as "Trojan horses" for migration to the T cell area (Reizis, 2011). However, cDCs may have evolved counteracting mechanisms to restrict their intracellular niche for live bacteria. Therefore, we wanted to study the importance of MyD88 signaling in this process. Indeed, a correlation for a MyD88-dependent increase in reactive oxygen species (ROS) production by the NADPH oxidase NOX2 and hence more efficient killing of Gram-negative bacteria has been established for mouse primary macrophages (Laroux et al., 2005) and human monocyte-derived DCs (Vulcano et al., 2004). More recently, it was shown

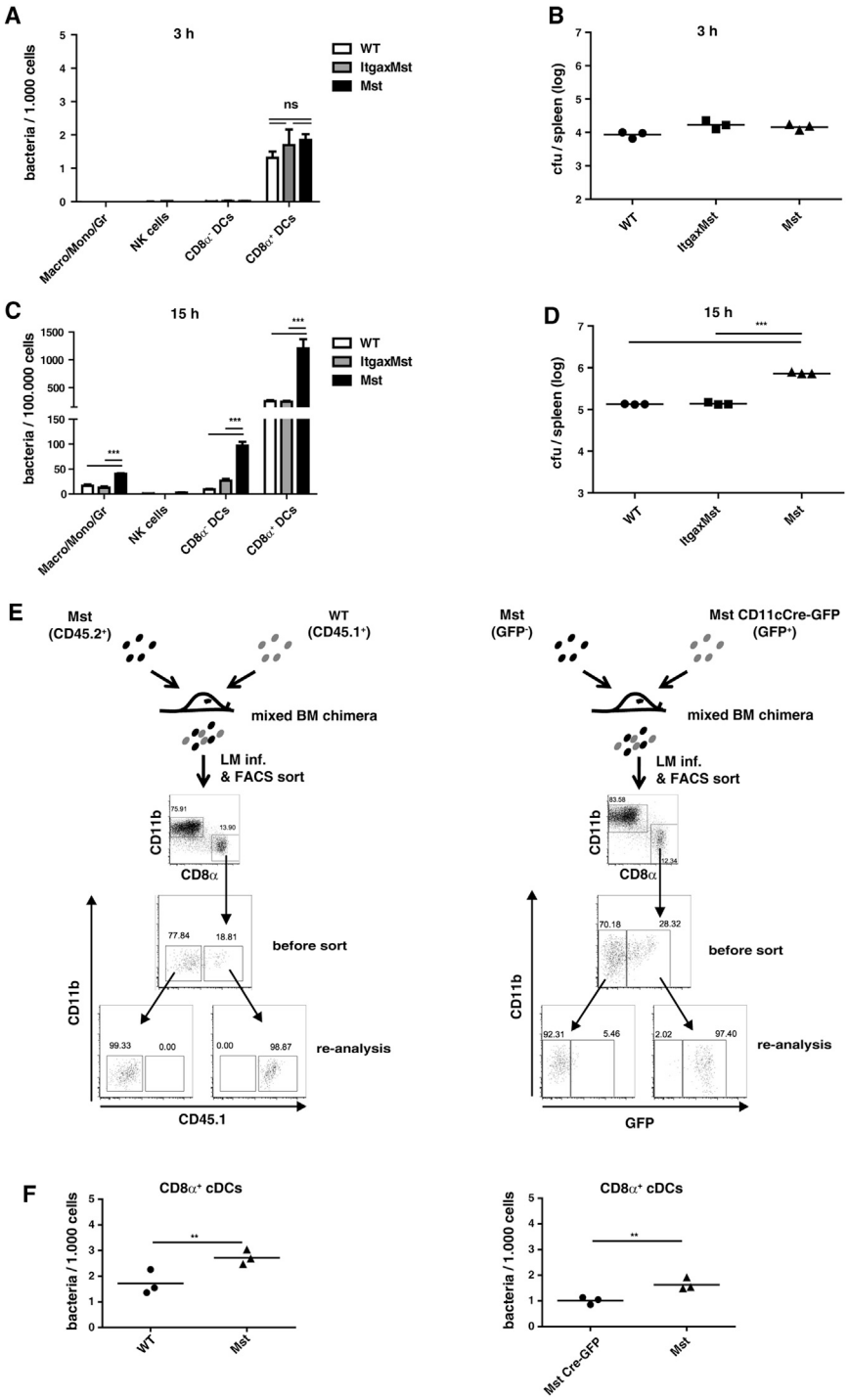

Figure 4. MyD88 Signaling Controls the Niche Size for Live LM in CD8α⁺ cDCs

(A and C) Mice were infected with LM and spleens were removed at (A) 3 hpi or (C) 15 hpi. The number of intracellular bacteria per 10^3 or 10^5 sorted macrophages/monocytes/granulocytes, NK cells, CD8α⁻ cDCs, or CD8α⁺ cDCs from pooled spleens is depicted. Data are shown as mean + SD.

(B and D) The bacterial burden/spleen of each group was determined at the indicated time points. Bars represent mean values. The experiments shown were repeated three times (A) or four times (C). Statistics were calculated by one-way ANOVA. ns, not significant.

(E) Mixed BM chimeras were generated using CD45.2⁺/GFP⁻ Mst BM in combination with CD45.1⁺ WT BM or GFP⁺ Mst CD11cCre-GFP BM. At 9 hpi, pooled spleens from infected chimeras were FACS sorted into CD45.1⁺ and CD45.1⁻ CD8α⁺ or CD8α⁻ cells (left panel), or into GFP⁺ and GFP⁻ CD8α⁺ or CD8α⁻ cells (right panel).

(F) The bacterial burden in individual subsets from (E) is shown as the number of bacteria per 10^3 cells. The infection rates of CD8α⁻ cDCs were below the detection limit and are not displayed. Bars represent mean values. This experiment was performed twice with comparable results. Statistics were calculated by using Student's t test.

See also Figure S3.

that stimulation of macrophages with bacterial TLR1, TLR2, and TLR4 agonists augments their bactericidal activity through mitochondrial ROS production (West et al., 2011). However, no studies have been performed by directly targeting cDCs in vivo. Surprisingly, in contrast to published data obtained with other phagocytes, we show that a deficiency in MyD88 signaling by ex vivo CD8α⁺ cDCs had no effect on their microbicidal activity during infection with the Gram-positive bacterium LM. This discrepancy might be explained by the fact that CD8α⁺ cDCs, in contrast to other phagocytes, require a constant neutral pH value in the phagolysosome as a prerequisite for efficient cross-presentation. In this process, NOX2 recycles protons from the vesicular ATPase to prevent acidification (Savina and Amigorena, 2007). It is an attractive hypothesis that the equilibrium between ROS production and proton consumption is also maintained upon infection and hence has little effect on bacterial killing. The absence of differences in the bacterial burden between ex vivo WT and MyD88-deficient CD8α⁺ cDCs suggests that the microbicidal capacity of CD8α⁺ cDCs could also be influenced by MyD88-independent pathways or negative regulation of TLR-induced activation, consequently leading to comparable killing activities in WT and Mst cDCs. Indeed, MyD88-independent innate receptors can recognize LM (Williams et al., 2012), and TLR-mediated signaling can be negatively regulated by the PRRs NOD2 (Watanabe et al., 2004) and NLRP6 (Anand et al., 2012), as shown in mouse macrophages. Thus, MyD88-dependent and -independent pathways might cooperate to fine-tune the bactericidal activity in splenic CD8α⁺ cDCs during LM infection.

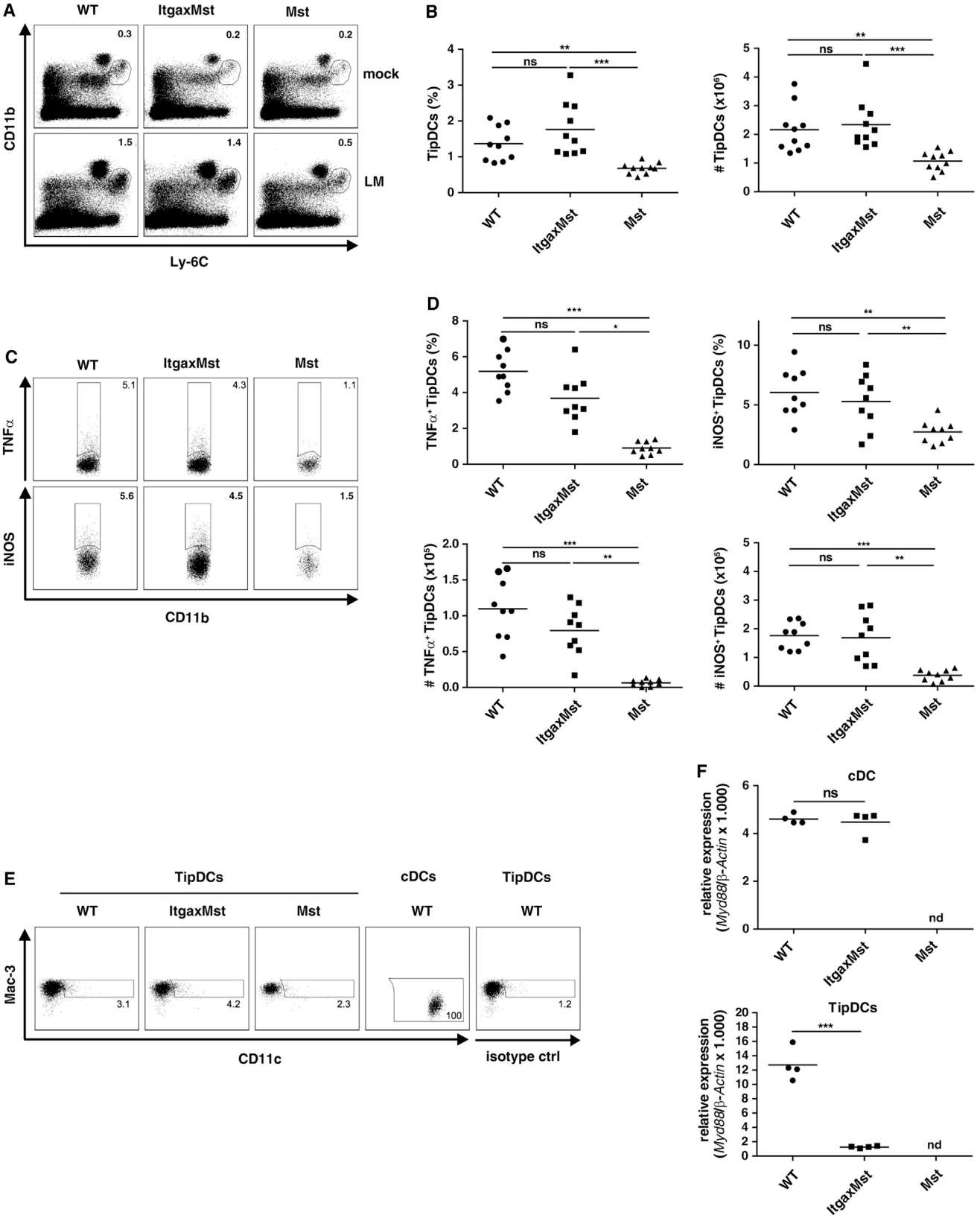

(legend on next page)

Our mouse model is based on the targeted expression of MyD88 specifically in DCs. Although MyD88 also functions as an adaptor protein downstream of the IL-1R family, there is substantial evidence in the literature that TLR-mediated signaling is more dominant for a functional innate immune response against LM. Deficiencies in Caspase1, ASC, IL-18, or IL-1R, which couple to the inflammasome pathway, do not contribute to increased susceptibility, and mice with these deficiencies show only a mild increase in bacterial burden as compared with *Myd88*$^{-/-}$ mice (Glaccum et al., 1997; Lochner et al., 2008; Sauer et al., 2011; Tsuji et al., 2004). Moreover, TipDC activation occurs independently of IL-1 and IL-18 signaling (Serbina et al., 2003a). Thus, also in our study TLR-mediated, rather than IL-1R-family-dependent, MyD88 signaling plays a major role in the induction of a protective innate immune response. However, which PRRs mediate MyD88-dependent activation is still under debate. For the systemic infection model, only TLR2 has been demonstrated to participate in LM recognition (Torres et al., 2004), probably due to heterodimerization with TLR1 or TLR6 (Ozinsky et al., 2000), as the deficiency in TLR2 activation does not fully recapitulate the defects observed in *Myd88*$^{-/-}$ mice. Data from in vivo experiments in *Tlr5*$^{-/-}$ or *Tlr9*$^{-/-}$ mice testing for the recognition of flagellin or bacterial DNA are not available. Furthermore, TLR13, a recently described receptor for bacterial ribosomal RNA recognition (Oldenburg et al., 2012), might be an interesting candidate to explain the differences in susceptibility to LM infection between *Tlr2*$^{-/-}$ and *Myd88*$^{-/-}$ mice.

Although in this study we focused on DCs, Yang et al. (2007) noted the importance of TLR signaling by macrophages during LM infection. In their study, mice deficient in expression of the chaperon gp96 by LysM^{+} cells (which leads to disruptive TLR2, TLR4, TLR5, TLR7, and TLR9 signaling in these cells) were infected with LM i.p. and displayed a higher bacterial burden and greater tissue damage as compared with WT mice. The authors concluded that TLR signaling by LysM^{+} macrophages is critically required for protection against LM. However, it is difficult to compare their findings with our data due to differences in the infectious routes and doses used. Also, Yang et al. (2007) did not provide a direct comparison of their transgenic mice and *Myd88*$^{-/-}$ mice, or the relative survival of both groups. Nevertheless, in our study, we do not exclude a contribution of TLR signaling by non-DCs in WT mice; rather, we postulate that TLR signaling by DCs is sufficient for innate immune activation against LM.

In our experimental approach, we aimed to target cDCs by using CD11cCre mice. However, we cannot formally rule out contributions of the effects of MyD88 signaling by other CD11c-expressing cells, such as NK cells and plasmacytoid DCs, to the observed phenotype. DCs, rather than macrophages, are required for NK cell activation during LM infection, and NK cells do not rely on cell-autonomous TLR signaling for IFNγ production (Kang et al., 2008; Lucas et al., 2007). Yet, the generation of alternative Cre mouse lines with refined specificities for cDCs or CD8α^{+} cDCs employing, e.g., the *Zbtb46*, *Clec9a*, or *Xcr1* (Dorner et al., 2009; Meredith et al., 2012; Satpathy et al., 2012; Schraml et al., 2013) promoter would be beneficial to confirm our results. In any case, the advantage of targeting DC genes rather than using a DC-depletion approach is that there is no interference with DC-mediated bacterial transport to the T cell area, a critical host-pathogen interaction during LM infection.

We have demonstrated that mice with a functional MyD88 signaling cascade specifically in DCs control their bacterial burden early during infection, in contrast to MyD88-deficient mice. To understand the mechanism behind this, we focused on studying the activation of inflammatory monocytes because they are key players in controlling early bacterial replication (Serbina et al., 2008; Shi et al., 2011) and express CD11c at intermediate levels when analyzed at 48 hpi (Serbina et al., 2003b). TipDC activation is MyD88 dependent, as demonstrated in *Myd88*$^{-/-}$ mice. This led to the hypothesis that TipDCs, which are poorly infected in vivo, require direct activation via pathogen-associated molecular patterns (Serbina et al., 2003a, 2003b). However, in our model, we found that at 24 hpi, intrinsic MyD88 signaling by TipDCs is not required for their activation during early infection with LM. cDCs provide the key cytokine IL-12, which is necessary for IFNγ-dependent TipDC activation during LM infection (Kang et al., 2008), and we demonstrated that IL-12 production by CD8α^{+} cDCs is functional at an earlier time point postinfection in ItgaxMst mice as compared with Mst mice. A recent study by Lee et al. (2013) unraveled an unexpected role of IFNγ receptor signaling in amplifying IL-12 production by CD8α^{+} cDCs. They showed that IL-12 production is reduced, but not abrogated, in the absence of DC-specific IFNγ receptor signaling. Thus, in line with our findings, it is most likely that CD8α^{+} cDCs produce the first IL-12 that initiates IFNγ production, as previously suggested for *Toxoplasma gondii* (Reis e Sousa et al., 1997; Mashayekhi et al., 2011). Moreover, Lee et al. (2013) demonstrated that IL-12 and IFNγ production partially

Figure 5. TipDCs Do Not Require Cell-Intrinsic MyD88 Signaling for their Activation

(A) Mice were infected with LM for 24 hr. TipDCs from uninfected and infected mice were gated as CD11b^{int}Ly-6C^{hi} as indicated. Representative live-cell gates from spleen are depicted. See also Figure S4.

(B) Quantification of the frequency and total numbers of TipDCs from infected mice gated as in (A). Pooled data from two independent experiments are depicted. The numbers of CD11b^{int}Ly-6C^{hi} cells were comparable in uninfected mice from all tested genotypes (mean value/spleen = 0.28 × 10^{6} cells; data not shown).

(C) Representative FACS plots showing TNF-α and iNOS expression by TipDCs gated as in (A).

(D) Quantification of the frequencies (upper panels) or total numbers (lower panels) of TipDCs from (C) positive for intracellular iNOS and TNF-α. Data were pooled from two independent experiments.

(E) CD11c/Mac-3 expression by gated live CD11b^{int}Ly-6C^{hi} cells or cDCs in comparison with the isotype control for the CD11c antibody.

(F) Quantitative RT-PCR for *Myd88* expression by FACS-sorted CD11b^{int} Ly-6C^{hi} TipDCs from infected WT and ItgaxMst mice. As control, CD11c^{hi} splenic cDCs were used. The graphs show pooled data from two independent experiments. Statistics were calculated by using Student's t test. Symbols in (B), (D), and (F) represent individual mice, and bars indicate mean values. ns, not significant; nd, not detectable.

depends on transmembrane TNF-α. DCs express membrane-bound TNF-α, which is required for DC/NK cell crosstalk (Xu et al., 2007), and DC/NK cell clusters are essential for IFNγ production upon LM infection (Kang et al., 2008). TNF-α could be presented by activated cDCs in LM-infected ItgaxMst mice. Thus, we suggest that upon LM infection, MyD88 signaling in DCs initiates both IL-12 and possibly transmembrane TNF-α expression.

We propose that an important function of cDCs during LM infection is to provide a critical backup mechanism for indirect TipDC activation. This mechanism might also be relevant for infections with other pathogens, such as *Brucella melitensis*, *Leishmania major*, *Mycobacterium tuberculosis*, and *Toxoplasma gondii*, where the activation of inflammatory monocytes also critically controls the pathogen burden during the innate immune response (Copin et al., 2007; De Trez et al., 2009; Peters et al., 2001; Robben et al., 2005). Taken together, our findings demonstrate that MyD88 signaling is sufficient in cDCs but dispensable in TipDCs for the induction of early innate responses against the intracellular pathogen LM in vivo.

EXPERIMENTAL PROCEDURES

Additional details regarding the materials and methods used in this work are provided in Supplemental Experimental Procedures.

Mice

All animal experiments were performed in compliance with the German animal protection law (TierSchG BGBl. I S. 1105; 25.05.1998) and approved by the Lower Saxony Committee on the Ethics of Animal Experiments as well as the responsible state office (Lower Saxony State Office of Consumer Protection and Food Safety). Mice were housed and handled in accordance with good animal practice as defined by FELASA and the national animal welfare body GV-SOLAS. Mice were bred at the TWINCORE and HZI animal facilities (Hannover/Braunschweig) under specific pathogen-free conditions. Mst mice were kindly provided by B. Holzmann (Gais et al., 2012), ItgaxCre mice (Caton et al., 2007) were provided by B. Reizis, and CD11cCre-GFP mice (Stranges et al., 2007) were provided by A.V. Chervonsky. All mice were on the C57Bl/6J background. Transgenic and WT mice from the ItgaxCre breedings were used as control mice.

To generate mixed BM chimeras, mice were irradiated with 10 Gy. BM cells were transferred i.v. the next day. Engraftment was assessed prior to experiments 6–8 weeks later in the blood. In WT/Mst BM chimeras, WT cells were identified by CD45.1 expression. In Mst CD11cCre-GFP/Mst chimeras, transgenic DCs were gated as GFP^+. DCs were expanded for fluorescence-activated cell sorting (FACS) experiments by injecting mice s.c. with an Flt3L-expressing B16 cell line kindly provided by M. O'Keeffe. Splenic DCs were harvested 12–14 days later. For some experiments, mice were injected with PBS or 10 nmol CpG-B 1826 (TibMolbio) in PBS i.p., and serum was collected 2 hr later and stored at −20°C until use.

Bacterial Culture and Infection

For infection studies, the LM 10403s OVA strain (Foulds et al., 2002) and the LM RFP strain generated on the DP-L4056 background (Waite et al., 2011; kindly provided by H. Shen or D.A. Portnoy) were used. LM was grown in Tryptic Soy Broth (TSB; BD Bioscience). For details on the bacterial cultures and preparation of heat-killed (HK) LM, see Supplemental Experimental Procedures. The following infectious doses (i.v.) of LM OVA were used: 5×10^3 cfu for survival curves and infection studies (24 and 72 hr); 5×10^4 cfu for TipDC/DC activation; and 5×10^5 cfu for sorting by FACS. For histology, mice were infected i.v. with 1×10^6 cfu LM RFP.

To determine the bacterial burden, organs were smashed in 1 ml PBS (GIBCO) in sterile bags (Nasco) to release intracellular bacteria. Alternatively, cells were resuspended in PBS and lysed by adding the same volume of 0.1% Triton X-100 (Sigma) in dH_20 followed by 5 s of vortexing. Serial dilutions of the organ/cell lysates were plated on TSB agar plates (BD Bioscience) containing 50 μg/ml erythromycin (Sigma; for the LM OVA strain) and incubated at +37°C for 48 hr.

Preparation of Splenocytes

Spleens were digested using collagenase D and DNase I (both from Roche) under constant pipetting (room temperature, 20 min). Reactions were stopped by adding 10 mM EDTA for 5 min. Red blood cell lysis (150 mM NH_4Cl, 10 mM $KHCO_3$, 0.1 mM EDTA; pH 7.2–7.4) was performed for 1 min (at room temperature) and stopped by adding 2% fetal calf serum (FCS)/RPMI 1640 Glutamax (GIBCO). Cells were incubated in 10% FCS, 50 μM β-mercaptoethanol (both Biochrom) in RPMI1640 Glutamax (GIBCO). Ex vivo DCs were enriched by a density gradient using Optiprep (Axis Shield) prior to FACS.

DC Cultures and Stimulations

GM-CSF DCs were generated according to a standard protocol (Lutz et al., 1999) and contained at least 80% of $CD11c^+$ cells on the day of the experiment. GM-CSF DCs (5×10^4) or FACS-sorted splenic cDCs (1×10^5) were stimulated with either 1 nmol/ml CpG-B 1826 (TIB Molbio), 10 μg/ml Pam3CSK4 (InvivoGen), a moi 1 of HK *C. albicans* strain 21:333–340 (heat inactivation for 1 hr at 96°C) (Barelle et al., 2004), a moi 100 of HK LM WT EGD, or 1.43 mg/ml γ-irradiated *M. tuberculosis* strain H37Rv (NR-14819; BEI Resources, NIAID, NIH) in a 96-well round-bottom plate.

The *C. albicans* strain was kindly provided by C. Reis e Sousa. After 24 hr (+37°C, 5% CO_2), supernatants were collected and analyzed for IL-12p40 or TNF-α using the DuoSet ELISA kits (R&D) and cells were used for FACS staining. To assess TipDC/cDC activation, splenocytes were digested (see above) in the presence of Golgi Plug (BD Bioscience). Prior to FACS staining, 10×10^6 cells were incubated (4 hr, +37°C, 5% CO_2) with or without 10^7 cfu/ml HK-LM OVA in the presence of 5 μg/ml gentamicin.

Immunofluorescent Microscopy

Organs were incubated in 30% sucrose in PBS (3–4 hr, +4°C), mounted in OCT medium (Tissue-Tek), frozen on dry ice, and stored at −80°C. Then 5 μm cryosections were cut with a CryostarNX70 cryostat (ThermoScientific). Dried sections were kept at −80°C until use and fixed with acetone (−20°C, 10 min). For details on the staining, see Supplemental Experimental Procedures. Microscopy was performed on an Axioskop 40FL fluorescence microscope using an AxioCamMRm camera and AxioVision Rel 4.8 software (all from Zeiss). LM RFP infection in the T cell areas was quantified as the number of RFP pixels/number of total pixels in the T cell area using ImageJ software (NIH).

Flow Cytometry

Calcium/magnesium-free PBS (GIBCO) containing 2 mM EDTA/0.5% BSA was used during the entire staining procedure. For details on the antibodies used, see Supplemental Experimental Procedures. Serum cytokines were measured using a multiplex bead assay kit (mouse flowCytomix; eBioscience). Dead cells were excluded by DAPI (Sigma), the LIVE/DEAD Fixable Aqua Dead Cell Stain Kit (Invitrogen), or ethidium bromide monoazide (Sigma) staining, and cellular aggregates were excluded by side-scatter pulse width. Cytometric acquisition/analysis was performed using LSRII (BD Bioscience) and FlowJo software (Treestar).

FACS

The FACS sorting experiments shown in Figure 4 were based on a published protocol (Neuenhahn et al., 2006). Briefly, spleens from infected mice were pooled and digested (see "Preparation of Splenocytes" above) in the presence of 5 μg/ml gentamicin (PAA) to kill extracellular bacteria. B cells were depleted with anti-B220 or anti-CD19 magnetic beads (Miltenyi). For staining and gating strategy details, see Supplemental Experimental Procedures. Single-cell suspensions were prepared using filter tubes (BD Bioscience). For functional assays, DCs were sorted with a 100 μm nozzle (otherwise 70 μm) using the FACS Aria (BD Bioscience) or XPD (Beckman Coulter) FACS sorters. Cells were collected in 1 ml FCS. The sorting purities were >95%–98%.

Real-Time PCR

Total RNA was isolated from FACS-sorted cells using the RNeasy kit (QIAGEN). cDNA was generated using Superscript III reverse transcriptase in the presence of RNaseOUT Recombinant Ribonuclease Inhibitor (both Invitrogen). For the primers used, see Supplemental Experimental Procedures. Both reactions were run at the Light Cycler 480 II (Roche) using the following protocol: 10 min at 95°C, 40 cycles of 15 s at 95°C and 1 min at 60°C, and cooling to 15°C. Melting curves were generated (15 s at 95°C, 15 s at 60°C, cont. at 95°C) for each sample. Relative *Myd88* expression was calculated as $[2^{-Ct\ (Myd88)} / 2^{-Ct\ (\beta\text{-}Actin)}]$.

Statistical Analysis

For survival curves, a log rank test was performed. All other statistical analyses were performed using one-way ANOVA with subsequent Newman-Keuls posttest, the Kruskal-Wallis test followed by Dunn's posttest, or Student's t test as indicated in the figure legends. Analysis was performed using GraphPad Prism software (*$p < 0.05$, **$p < 0.01$, ***$p < 0.001$).

SUPPLEMENTAL INFORMATION

Supplemental Information includes Supplemental Experimental Procedures and four figures and can be found with this article online at http://dx.doi.org/10.1016/j.celrep.2014.01.023.

ACKNOWLEDGMENTS

We thank S. Dippel, E. Ermeling, and C. Jänke for expert technical support. We also thank H.W. Mittrücker, P. Dresing, and S. Scheu for initial support with the *Listeria* infection model and J. Hühn, S. Halle, S. Cording, and S. Amigorena for helpful discussions. Finally, we acknowledge the assistance of the Cell Sorting Core Facility of the Hannover Medical School, supported in part by Braukmann-Wittenberg-Herz-Stiftung and the Deutsche Forschungsgemeinschaft (DFG). C.A.S. received a PhD stipend as well as personal support from the Boehringer Ingelheim Fonds, Foundation for Basic Research in Medicine. M.D. received a PhD stipend from the DFG in the framework of the International Research Training Group (IRTG) 1273. This project was financed by SFB900.

Received: October 18, 2013
Revised: December 19, 2013
Accepted: January 17, 2014
Published: February 13, 2014

REFERENCES

Akira, S., and Takeda, K. (2004). Toll-like receptor signalling. Nat. Rev. Immunol. *4*, 499–511.

Alaniz, R.C., Sandall, S., Thomas, E.K., and Wilson, C.B. (2004). Increased dendritic cell numbers impair protective immunity to intracellular bacteria despite augmenting antigen-specific CD8+ T lymphocyte responses. J. Immunol. *172*, 3725–3735.

Anand, P.K., Malireddi, R.K., Lukens, J.R., Vogel, P., Bertin, J., Lamkanfi, M., and Kanneganti, T.D. (2012). NLRP6 negatively regulates innate immunity and host defence against bacterial pathogens. Nature *488*, 389–393.

Aoshi, T., Zinselmeyer, B.H., Konjufca, V., Lynch, J.N., Zhang, X., Koide, Y., and Miller, M.J. (2008). Bacterial entry to the splenic white pulp initiates antigen presentation to CD8+ T cells. Immunity *29*, 476–486.

Aoshi, T., Carrero, J.A., Konjufca, V., Koide, Y., Unanue, E.R., and Miller, M.J. (2009). The cellular niche of Listeria monocytogenes infection changes rapidly in the spleen. Eur. J. Immunol. *39*, 417–425.

Barelle, C.J., Manson, C.L., MacCallum, D.M., Odds, F.C., Gow, N.A., and Brown, A.J. (2004). GFP as a quantitative reporter of gene regulation in Candida albicans. Yeast *21*, 333–340.

Campisi, L., Soudja, S.M., Cazareth, J., Bassand, D., Lazzari, A., Brau, F., Narni-Mancinelli, E., Glaichenhaus, N., Geissmann, F., and Lauvau, G. (2011). Splenic CD8α$^+$ dendritic cells undergo rapid programming by cytosolic bacteria and inflammation to induce protective CD8$^+$ T-cell memory. Eur. J. Immunol. *41*, 1594–1605.

Caton, M.L., Smith-Raska, M.R., and Reizis, B. (2007). Notch-RBP-J signaling controls the homeostasis of CD8- dendritic cells in the spleen. J. Exp. Med. *204*, 1653–1664.

Connolly, D.J., and O'Neill, L.A. (2012). New developments in Toll-like receptor targeted therapeutics. Curr. Opin. Pharmacol. *12*, 510–518.

Copin, R., De Baetselier, P., Carlier, Y., Letesson, J.J., and Muraille, E. (2007). MyD88-dependent activation of B220-CD11b+LY-6C+ dendritic cells during Brucella melitensis infection. J. Immunol. *178*, 5182–5191.

De Trez, C., Magez, S., Akira, S., Ryffel, B., Carlier, Y., and Muraille, E. (2009). iNOS-producing inflammatory dendritic cells constitute the major infected cell type during the chronic Leishmania major infection phase of C57BL/6 resistant mice. PLoS Pathog. *5*, e1000494.

Dorner, B.G., Dorner, M.B., Zhou, X., Opitz, C., Mora, A., Güttler, S., Hutloff, A., Mages, H.W., Ranke, K., Schaefer, M., et al. (2009). Selective expression of the chemokine receptor XCR1 on cross-presenting dendritic cells determines cooperation with CD8+ T cells. Immunity *31*, 823–833.

Edelson, B.T., and Unanue, E.R. (2002). MyD88-dependent but Toll-like receptor 2-independent innate immunity to Listeria: no role for either in macrophage listericidal activity. J. Immunol. *169*, 3869–3875.

Edelson, B.T., Bradstreet, T.R., Hildner, K., Carrero, J.A., Frederick, K.E., Kc, W., Belizaire, R., Aoshi, T., Schreiber, R.D., Miller, M.J., et al. (2011). CD8α(+) dendritic cells are an obligate cellular entry point for productive infection by Listeria monocytogenes. Immunity *35*, 236–248.

Foulds, K.E., Zenewicz, L.A., Shedlock, D.J., Jiang, J., Troy, A.E., and Shen, H. (2002). Cutting edge: CD4 and CD8 T cells are intrinsically different in their proliferative responses. J. Immunol. *168*, 1528–1532.

Gais, P., Reim, D., Jusek, G., Rossmann-Bloeck, T., Weighardt, H., Pfeffer, K., Altmayr, F., Janssen, K.P., and Holzmann, B. (2012). Cutting edge: Divergent cell-specific functions of MyD88 for inflammatory responses and organ injury in septic peritonitis. J. Immunol. *188*, 5833–5837.

Glaccum, M.B., Stocking, K.L., Charrier, K., Smith, J.L., Willis, C.R., Maliszewski, C., Livingston, D.J., Peschon, J.J., and Morrissey, P.J. (1997). Phenotypic and functional characterization of mice that lack the type I receptor for IL-1. J. Immunol. *159*, 3364–3371.

Hemmi, H., Takeuchi, O., Kawai, T., Kaisho, T., Sato, S., Sanjo, H., Matsumoto, M., Hoshino, K., Wagner, H., Takeda, K., and Akira, S. (2000). A Toll-like receptor recognizes bacterial DNA. Nature *408*, 740–745.

Kang, S.J., Liang, H.E., Reizis, B., and Locksley, R.M. (2008). Regulation of hierarchical clustering and activation of innate immune cells by dendritic cells. Immunity *29*, 819–833.

Laroux, F.S., Romero, X., Wetzler, L., Engel, P., and Terhorst, C. (2005). Cutting edge: MyD88 controls phagocyte NADPH oxidase function and killing of gram-negative bacteria. J. Immunol. *175*, 5596–5600.

Lee, S.H., Carrero, J.A., Uppaluri, R., White, J.M., Archambault, J.M., Lai, K.S., Chan, S.R., Sheehan, K.C., Unanue, E.R., and Schreiber, R.D. (2013). Identifying the initiating events of anti-Listeria responses using mice with conditional loss of IFN-γ receptor subunit 1 (IFNGR1). J. Immunol. *191*, 4223–4234.

Lochner, M., Kastenmüller, K., Neuenhahn, M., Weighardt, H., Busch, D.H., Reindl, W., and Förster, I. (2008). Decreased susceptibility of mice to infection with Listeria monocytogenes in the absence of interleukin-18. Infect. Immun. *76*, 3881–3890.

Lucas, M., Schachterle, W., Oberle, K., Aichele, P., and Diefenbach, A. (2007). Dendritic cells prime natural killer cells by trans-presenting interleukin 15. Immunity *26*, 503–517.

Lutz, M.B., Kukutsch, N., Ogilvie, A.L., Rössner, S., Koch, F., Romani, N., and Schuler, G. (1999). An advanced culture method for generating large quantities of highly pure dendritic cells from mouse bone marrow. J. Immunol. Methods *223*, 77–92.

Mashayekhi, M., Sandau, M.M., Dunay, I.R., Frickel, E.M., Khan, A., Goldszmid, R.S., Sher, A., Ploegh, H.L., Murphy, T.L., Sibley, L.D., and Murphy,

K.M. (2011). CD8α(+) dendritic cells are the critical source of interleukin-12 that controls acute infection by Toxoplasma gondii tachyzoites. Immunity *35*, 249–259.

Meredith, M.M., Liu, K., Darrasse-Jeze, G., Kamphorst, A.O., Schreiber, H.A., Guermonprez, P., Idoyaga, J., Cheong, C., Yao, K.H., Niec, R.E., and Nussenzweig, M.C. (2012). Expression of the zinc finger transcription factor zDC (Zbtb46, Btbd4) defines the classical dendritic cell lineage. J. Exp. Med. *209*, 1153–1165.

Neuenhahn, M., Kerksiek, K.M., Nauerth, M., Suhre, M.H., Schiemann, M., Gebhardt, F.E., Stemberger, C., Panthel, K., Schröder, S., Chakraborty, T., et al. (2006). CD8alpha+ dendritic cells are required for efficient entry of Listeria monocytogenes into the spleen. Immunity *25*, 619–630.

Oldenburg, M., Krüger, A., Ferstl, R., Kaufmann, A., Nees, G., Sigmund, A., Bathke, B., Lauterbach, H., Suter, M., Dreher, S., et al. (2012). TLR13 recognizes bacterial 23S rRNA devoid of erythromycin resistance-forming modification. Science *337*, 1111–1115.

Ozinsky, A., Underhill, D.M., Fontenot, J.D., Hajjar, A.M., Smith, K.D., Wilson, C.B., Schroeder, L., and Aderem, A. (2000). The repertoire for pattern recognition of pathogens by the innate immune system is defined by cooperation between toll-like receptors. Proc. Natl. Acad. Sci. USA *97*, 13766–13771.

Pamer, E.G. (2004). Immune responses to Listeria monocytogenes. Nat. Rev. Immunol. *4*, 812–823.

Peters, W., Scott, H.M., Chambers, H.F., Flynn, J.L., Charo, I.F., and Ernst, J.D. (2001). Chemokine receptor 2 serves an early and essential role in resistance to Mycobacterium tuberculosis. Proc. Natl. Acad. Sci. USA *98*, 7958–7963.

Reis e Sousa, C., Hieny, S., Scharton-Kersten, T., Jankovic, D., Charest, H., Germain, R.N., and Sher, A. (1997). In vivo microbial stimulation induces rapid CD40 ligand-independent production of interleukin 12 by dendritic cells and their redistribution to T cell areas. J. Exp. Med. *186*, 1819–1829.

Reizis, B. (2011). Intracellular pathogens and CD8(+) dendritic cells: dangerous liaisons. Immunity *35*, 153–155.

Robben, P.M., LaRegina, M., Kuziel, W.A., and Sibley, L.D. (2005). Recruitment of Gr-1+ monocytes is essential for control of acute toxoplasmosis. J. Exp. Med. *201*, 1761–1769.

Sathaliyawala, T., O'Gorman, W.E., Greter, M., Bogunovic, M., Konjufca, V., Hou, Z.E., Nolan, G.P., Miller, M.J., Merad, M., and Reizis, B. (2010). Mammalian target of rapamycin controls dendritic cell development downstream of Flt3 ligand signaling. Immunity *33*, 597–606.

Satpathy, A.T., Kc, W., Albring, J.C., Edelson, B.T., Kretzer, N.M., Bhattacharya, D., Murphy, T.L., and Murphy, K.M. (2012). Zbtb46 expression distinguishes classical dendritic cells and their committed progenitors from other immune lineages. J. Exp. Med. *209*, 1135–1152.

Sauer, J.D., Pereyre, S., Archer, K.A., Burke, T.P., Hanson, B., Lauer, P., and Portnoy, D.A. (2011). Listeria monocytogenes engineered to activate the Nlrc4 inflammasome are severely attenuated and are poor inducers of protective immunity. Proc. Natl. Acad. Sci. USA *108*, 12419–12424.

Savina, A., and Amigorena, S. (2007). Phagocytosis and antigen presentation in dendritic cells. Immunol. Rev. *219*, 143–156.

Schraml, B.U., van Blijswijk, J., Zelenay, S., Whitney, P.G., Filby, A., Acton, S.E., Rogers, N.C., Moncaut, N., Carvajal, J.J., and Reis e Sousa, C. (2013). Genetic tracing via DNGR-1 expression history defines dendritic cells as a hematopoietic lineage. Cell *154*, 843–858.

Seki, E., Tsutsui, H., Tsuji, N.M., Hayashi, N., Adachi, K., Nakano, H., Futatsugi-Yumikura, S., Takeuchi, O., Hoshino, K., Akira, S., et al. (2002). Critical roles of myeloid differentiation factor 88-dependent proinflammatory cytokine release in early phase clearance of Listeria monocytogenes in mice. J. Immunol. *169*, 3863–3868.

Serbina, N.V., Kuziel, W., Flavell, R., Akira, S., Rollins, B., and Pamer, E.G. (2003a). Sequential MyD88-independent and -dependent activation of innate immune responses to intracellular bacterial infection. Immunity *19*, 891–901.

Serbina, N.V., Salazar-Mather, T.P., Biron, C.A., Kuziel, W.A., and Pamer, E.G. (2003b). TNF/iNOS-producing dendritic cells mediate innate immune defense against bacterial infection. Immunity *19*, 59–70.

Serbina, N.V., Jia, T., Hohl, T.M., and Pamer, E.G. (2008). Monocyte-mediated defense against microbial pathogens. Annu. Rev. Immunol. *26*, 421–452.

Shi, C., Hohl, T.M., Leiner, I., Equinda, M.J., Fan, X., and Pamer, E.G. (2011). Ly6G+ neutrophils are dispensable for defense against systemic Listeria monocytogenes infection. J. Immunol. *187*, 5293–5298.

Sparwasser, T., and Lipford, G.B. (2000). Consequences of bacterial CpG DNA-driven activation of antigen-presenting cells. Curr. Top. Microbiol. Immunol. *247*, 59–75.

Stavru, F., Archambaud, C., and Cossart, P. (2011). Cell biology and immunology of Listeria monocytogenes infections: novel insights. Immunol. Rev. *240*, 160–184.

Stranges, P.B., Watson, J., Cooper, C.J., Choisy-Rossi, C.M., Stonebraker, A.C., Beighton, R.A., Hartig, H., Sundberg, J.P., Servick, S., Kaufmann, G., et al. (2007). Elimination of antigen-presenting cells and autoreactive T cells by Fas contributes to prevention of autoimmunity. Immunity *26*, 629–641.

Tam, M.A., and Wick, M.J. (2006). Differential expansion, activation and effector functions of conventional and plasmacytoid dendritic cells in mouse tissues transiently infected with Listeria monocytogenes. Cell. Microbiol. *8*, 1172–1187.

Torres, D., Barrier, M., Bihl, F., Quesniaux, V.J., Maillet, I., Akira, S., Ryffel, B., and Erard, F. (2004). Toll-like receptor 2 is required for optimal control of Listeria monocytogenes infection. Infect. Immun. *72*, 2131–2139.

Tsuji, N.M., Tsutsui, H., Seki, E., Kuida, K., Okamura, H., Nakanishi, K., and Flavell, R.A. (2004). Roles of caspase-1 in Listeria infection in mice. Int. Immunol. *16*, 335–343.

van den Berg, L.M., Gringhuis, S.I., and Geijtenbeek, T.B. (2012). An evolutionary perspective on C-type lectins in infection and immunity. Ann. N Y Acad. Sci. *1253*, 149–158.

Verschoor, A., Neuenhahn, M., Navarini, A.A., Graef, P., Plaumann, A., Seidlmeier, A., Nieswandt, B., Massberg, S., Zinkernagel, R.M., Hengartner, H., and Busch, D.H. (2011). A platelet-mediated system for shuttling blood-borne bacteria to CD8α+ dendritic cells depends on glycoprotein GPIb and complement C3. Nat. Immunol. *12*, 1194–1201.

Vulcano, M., Dusi, S., Lissandrini, D., Badolato, R., Mazzi, P., Riboldi, E., Borroni, E., Calleri, A., Donini, M., Plebani, A., et al. (2004). Toll receptor-mediated regulation of NADPH oxidase in human dendritic cells. J. Immunol. *173*, 5749–5756.

Waite, J.C., Leiner, I., Lauer, P., Rae, C.S., Barbet, G., Zheng, H., Portnoy, D.A., Pamer, E.G., and Dustin, M.L. (2011). Dynamic imaging of the effector immune response to listeria infection in vivo. PLoS Pathog. *7*, e1001326.

Watanabe, T., Kitani, A., Murray, P.J., and Strober, W. (2004). NOD2 is a negative regulator of Toll-like receptor 2-mediated T helper type 1 responses. Nat. Immunol. *5*, 800–808.

West, A.P., Brodsky, I.E., Rahner, C., Woo, D.K., Erdjument-Bromage, H., Tempst, P., Walsh, M.C., Choi, Y., Shadel, G.S., and Ghosh, S. (2011). TLR signalling augments macrophage bactericidal activity through mitochondrial ROS. Nature *472*, 476–480.

Williams, M.A., Schmidt, R.L., and Lenz, L.L. (2012). Early events regulating immunity and pathogenesis during Listeria monocytogenes infection. Trends Immunol. *33*, 488–495.

Xu, J., Chakrabarti, A.K., Tan, J.L., Ge, L., Gambotto, A., and Vujanovic, N.L. (2007). Essential role of the TNF-TNFR2 cognate interaction in mouse dendritic cell-natural killer cell crosstalk. Blood *109*, 3333–3341.

Yang, Y., Liu, B., Dai, J., Srivastava, P.K., Zammit, D.J., Lefrançois, L., and Li, Z. (2007). Heat shock protein gp96 is a master chaperone for toll-like receptors and is important in the innate function of macrophages. Immunity *26*, 215–226.

Zhan, Y., Xu, Y., Seah, S., Brady, J.L., Carrington, E.M., Cheers, C., Croker, B.A., Wu, L., Villadangos, J.A., and Lew, A.M. (2010). Resident and monocyte-derived dendritic cells become dominant IL-12 producers under different conditions and signaling pathways. J. Immunol. *185*, 2125–2133.